

# High-Throughput Screening of Enzymes by Retroviral Display Using Droplet-Based Microfluidics

Lucia Granieri,<sup>1,2</sup> Jean-Christophe Baret,<sup>1,2</sup> Andrew D. Griffiths,<sup>1,2,\*</sup> and Christoph A. Merten<sup>1,2,\*</sup>

<sup>1</sup>Institut de Science et d'Ingénierie Supramoléculaires, Université de Strasbourg, 8 allée Gaspard Monge, 67083 Strasbourg Cedex, France

<sup>2</sup>Centre National de la Recherche Scientifique UMR 7006, 8 allée Gaspard Monge, 67083 Strasbourg Cedex, France

\*Correspondence: [cmerten@unistra.fr](mailto:cmerten@unistra.fr) (C.A.M.), [griffiths@unistra.fr](mailto:griffiths@unistra.fr) (A.D.G.)

DOI 10.1016/j.chembiol.2010.02.011

## SUMMARY

During the last 25 years, display techniques such as phage display have become very powerful tools for protein engineering, especially for the selection of monoclonal antibodies. However, while this method is extremely efficient for affinity-based selections, its use for the selection and directed evolution of enzymes is still very restricted. Furthermore, phage display is not suited for the engineering of mammalian proteins that require posttranslational modifications such as glycosylation or membrane anchoring. To circumvent these limitations, we have developed a system in which structurally complex mammalian enzymes are displayed on the surface of retroviruses and encapsulated into droplets of a water-in-oil emulsion. These droplets are made and manipulated using microfluidic devices and each droplet serves as an independent reaction vessel. Compartmentalization of single retroviral particles in droplets allows efficient coupling of genotype and phenotype. Using tissue plasminogen activator (tPA) as a model enzyme, we show that, by monitoring the enzymatic reaction in each droplet (by fluorescence), quantitative measurement of tPA activity in the presence of different concentrations of the endogenous inhibitor PAI-1 can be made on-chip. On-chip fluorescence-activated droplet sorting allowed the processing of 500 samples per second and the specific collection of retroviruses displaying active wild-type tPA from a model library with a 1000-fold excess of retroviruses displaying a non-active control enzyme. During a single selection cycle, a more than 1300-fold enrichment of the active wild-type enzyme was demonstrated.

## INTRODUCTION

Display technologies such as phage display are widely used techniques for protein engineering, allowing the selection and evolution of protein variants with desired properties (Levin and

Weiss, 2006). In a typical phage display experiment, huge numbers (up to  $10^{10}$ – $10^{12}$ ) of protein variants are generated on the genetic level and subsequently displayed fused to the coat proteins of phage particles. Phage particles package the gene encoding the protein variant displayed on their surface, which allows coupling of genotype and phenotype to be achieved. Subsequently these particles are subjected to a selection procedure (most commonly the binding to an immobilized target molecule). The power of this approach results from the fact that the phage can be replicated to allow multiple rounds of selection and directed evolution (if mutations are introduced between the rounds of selection). Furthermore, the generation of the libraries, as well as the amplification/identification of selected variants, can be performed using highly efficient genetic methods. This not only allows the rapid generation of billions of protein variants but also their selection and identification at concentrations that are far below the detection level of conventional methods in protein chemistry. These conceptual advantages have also been exploited by further display methods such as the display of proteins on the surface of bacteria (Francisco et al., 1993) or yeast cells (Boder and Wittrup, 1997) or completely in vitro systems such as ribosome (Hanes and Pluckthun, 1997) and mRNA display (Roberts and Szostak, 1997), where all steps of the selection procedure (including the protein expression) can be performed without the need for any cell transformation, thus allowing the screening of even more diverse libraries.

Phage display has been successfully used for the selection of therapeutic antibodies that are now in clinical use (e.g., the anti-TNF- $\alpha$  antibody Humira). Furthermore, the method has proven to be extremely powerful for the selection of other target-binding molecules such as ankyrin repeat proteins (Binz et al., 2003) and for the characterization of HIV protease cleavage sites (Beck et al., 2000). Phage display has also been used for the selection of proteins with catalytic activities. However, this application requires a technique coupling a catalytic property with an acquired binding activity. This can be achieved by displaying enzyme variants on the phage particles and subsequently selecting for binding to enzyme inhibitors or transition state analogs (Soumillion et al., 1994; Hansson et al., 1997). Alternatively, the enzyme and its substrate can be co-displayed on the phage particle before selecting for product-specific adsorption to a solid support (Demartis et al., 1999). However, these strategies and others generally do not allow the selection for multiple turnover (Fernandez-Gacio et al., 2003). Therefore,

enzyme variants that perform the desired chemical modification at very slow turnover rates (e.g., due to inefficient product release) are often selected (Vanwetswinkel et al., 2000). Consequently, the selection of efficient catalysts remains problematic when using phage particles.

Some cell-based strategies have been developed that allow this limitation to be circumvented. For example, enzyme variants can be displayed on the surface of the positively charged bacterial membrane. Hence negatively charged reaction products (generated from soluble fluorogenic substrates) attach to the surface and can thus be used to quantitatively determine the substrate turnover in fluorescence activated cell sorting experiments (Olsen et al., 2000). Alternatively, covalent binding of the fluorescent reaction product can be achieved when using specific acceptor molecules on the cellular membrane of yeast cells (Lipovsek et al., 2007). However, both strategies require specific chemical labels for the attachment of the reaction product (in addition to the fluorescent label) and are hence not truly generic.

We present here a novel approach for the screening of surface-displayed enzymes under multiple turnover conditions. In this system, enzymes are displayed on the surface of the murine leukemia virus (MLV) (Buchholz et al., 1998) and subsequently encapsulated into drops of a water-in-oil emulsion. Earlier studies have shown that each droplet can serve as an independent microreactor (Tawfik and Griffiths, 1998), allowing the selection of RNAs and proteins for a range of binding, regulatory, and catalytic activities (Griffiths and Tawfik, 2006). For example, enzymes can be selected under multiple turnover conditions using fluorogenic assays and sorting droplets triggered on fluorescence using either conventional fluorescence activated cell sorters (Mastrobattista et al., 2005; Aharoni et al., 2005) or microfluidic devices (Baret et al., 2009). In our system, we combine the power of microfluidic systems with eukaryotic virus display, which allows the screening of structurally complex proteins requiring disulfide bridging, glycosylation, and/or membrane anchorage. As a model system, we chose human tissue plasminogen activator (tPA), since this enzyme is of high therapeutic relevance (tPA is an emergency drug for deep vein strokes) and requires posttranslational modifications for enzymatic activity (Walsh and Jefferis, 2006).

## RESULTS

The goal of this work was the establishment of a novel method suitable for the directed evolution of structurally complex mammalian enzymes under multiple turnover conditions. In general, multiple turnover conditions can be achieved using in vitro compartmentalization, a technique in which proteins are translated within aqueous droplets of a water-in-oil emulsion (Tawfik and Griffiths, 1998). Each droplet then serves as an independent reaction vessel, thus allowing the use of soluble substrates and the selection for catalytic activity under multiple turnover conditions. However, as with phage display, this method is not well suited for mammalian enzymes like tPA, requiring comprehensive posttranslational modifications. The expression of unglycosylated but active tPA under oxidizing conditions in the periplasm of *Escherichia coli* has been demonstrated after coexpression of eukaryotic folding enzymes (Qiu et al., 1998).

However, we observed that in vitro-translated tPA is not active, unless translated under oxidizing conditions with simultaneous dialysis to allow disulfide bond formation (see Figure S1 available online). This procedure cannot be performed in aqueous microcompartments, for which reason we chose a different expression system. The MLV seemed to be perfectly suited since it allows expression of secreted, disulfide bonded, and glycosylated proteins in a eukaryotic context. To display the protein on the particle surface, we fused it N-terminally to the platelet-derived growth factor receptor transmembrane domain. Earlier studies had shown that the resulting fusion proteins are incorporated highly efficiently into MLV particles (Nikles et al., 2005). Furthermore, displaying the enzyme of interest directly on a nonviral transmembrane domain instead of the viral envelope protein rendered it resistant to shedding during particle concentration (the viral envelope protein consists of two noncovalently linked subunits partially dissociating during ultracentrifugation) (Yu and Wong, 1992). To guarantee the coupling of genotype and phenotype, an MLV-packagable vector was used for the expression of the fusion protein. Consequently, MLV particles displaying tPA on their surface and having packaged the encoding vector were obtained (MLV-tPA). For control purposes, we also generated particles displaying a non-related control enzyme (neuraminidase) and having packaged a distinguishable genetic marker (MLV-NA).

In the next step, we focused on coupling a fluorescence signal with catalytic activity. The reaction catalyzed by tPA is the cleavage of inactive plasminogen into active plasmin. Hence tPA activity can be monitored by either using a fluorescent tPA substrate or by using a fluorescent substrate for plasmin (Figure 1). This latter approach seemed to be preferable, since it allows screening using the physiological tPA substrate. Bulk experiments (using a plate reader) confirmed that MLV-tPA particles indeed generated a strong fluorescence signal using this assay. In contrast, the MLV-NA particles produced a very low background signal, thus confirming the specific monitoring of tPA activity (Figure S2). Noteworthy, when whole cells were used in the assay (instead of purified MLV particles), the generation of a significant fluorescence signal did not depend on the expression of tPA. Probably due to unspecific conversion of the substrate by other cellular enzymes, even wild-type HEK293T cells showed a significant fluorescence signal (Figure S2). This suggests that in vitro selection systems (such as phage or retrovirus display) might be better suited for enzyme evolution than their in vivo counterparts based on cell surface display.

As the next step, we used a microfluidic device (Figure 2A) to encapsulate the MLV-tPA particles together with all assay components into aqueous droplets (volume = 12 pL) of a water-in-oil emulsion. This step was performed in the presence of different concentrations of the endogenous inhibitor PAI-1 (0.5–4 µg/ml). As an internal reference, we spiked each emulsion additionally with droplets containing no inhibitor (produced by the second drop maker on the device; Figure 2A). The resulting emulsions were collected off-chip and incubated for 6 hr at 37°C before they were reinjected into a readout module (Figure 2B). A laser beam was focused onto the channels and the epifluorescence of each drop was recorded (processing 500 samples per second). As expected, we obtained three different

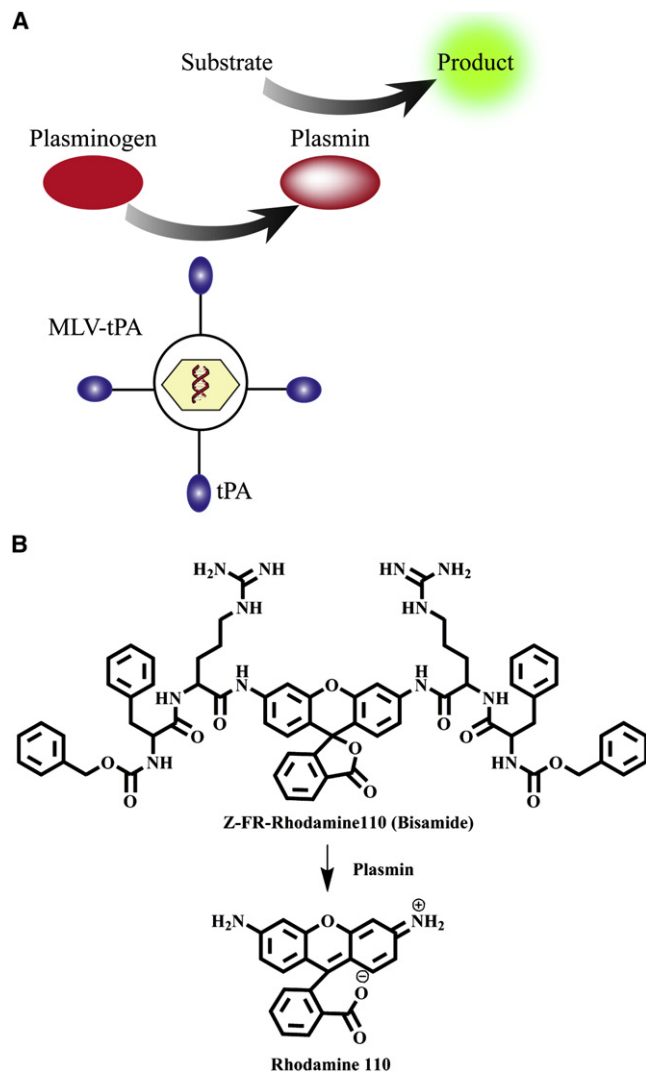


**Figure 1. Assay for the Enzymatic Activity of tPA**

(A) The enzyme is displayed on the surface of MLV particles and cleaves plasminogen into active plasmin, which in turn converts a non-fluorescent substrate into a fluorescent product.

(B) Chemical structure of the substrate and the fluorescent product.

populations in terms of the fluorescence intensity for each emulsion: the most negative population corresponds to droplets that do not host any MLV-tPA particle (to avoid multiple particles per drop on average only one particle per three drops was encapsulated), the population with an intermediate intensity corresponds to drops hosting an MLV-tPA particle in the presence of the inhibitor, and the most positive population corresponds to drops hosting an MLV-tPA particle in absence of any inhibitor (additional drops from the second drop maker). Having a defined positive and negative population for each emulsion allowed the fluorescence data of all samples to be normalized, enabling quantitative analysis of inhibition. As expected, increasing concentrations of PAI-1 resulted in decreasing fluorescence signals (Figure 3A). Analysis of the kinetic data (using GraphPad Prism) revealed an  $IC_{50}$  of 1.1  $\mu\text{g}/\text{ml}$  (Figure 3B),

which is in good agreement with bulk control experiments performed in a microplate reader ( $IC_{50} = 2.7 \mu\text{g}/\text{ml}$ ; data not shown). Furthermore, for all tested inhibitor concentrations, a peak well separated from the positive and negative population was obtained. This clearly demonstrates that this system is capable of discriminating populations with only small differences in their enzymatic activity.

In a further experiment we demonstrated the possibility of specifically enriching particles displaying active enzyme variants. For this purpose we generated mixtures of MLV-tPA particles (active) and MLV-NA particles (inactive) in a ratio of 1:100 and 1:1000. Using a microfluidic device (Figure 2C) these particle mixtures were encapsulated together with all assay components at the single particle level (approximately one particle per three drops). After 6 hr off-chip incubation at 37°C, the emulsions were reinjected into a microfluidic device designed for dielectrophoretic sorting of droplets (Ahn et al., 2006; Baret et al., 2009) (Figure 2D) and the fluorescence intensity of each drop was determined. For both mixtures, two distinct populations were obtained corresponding to empty droplets or droplets hosting MLV-NA particles (negative population) and droplets hosting MLV-tPA particles (positive population; Figure 4). In both the 1:100 and 1:1000 mixtures the percentage of positive drops was very close to that expected (1.3% and 0.3% of all drops, respectively; on average less than 7.5% of the droplets had coalesced) (Figures 4B and 4C). The sorting gates (red rectangles in Figures 4B and 4C) were set to include solely high fluorescence, non-coalesced drops (coalesced drops show a higher peak width and can therefore be excluded). The definition of the peak width (the time a fluorescence signal is above a certain threshold) results in highly fluorescent (positive) drops appearing slightly bigger than low fluorescence (negative) drops. However, this phenomenon is well understood and does not interfere with the gating for non-coalesced positive drops (Clausell-Tormos et al., 2008). Droplets flowed down the wider “negative” arm of the sorting junction by default due to its lower hydraulic resistance. However, when a droplet fell in the sorting gate, a pulse of high-voltage alternating current was applied across the electrodes adjacent to the sorting junction. The resulting electric field deflected the droplet of interest into the narrower “positive” arm of the junction by dielectrophoresis (Baret et al., 2009). For both mixtures, approximately 3500 positive droplets were collected.

Based on the genetic markers of the two particle species (MLV-tPA and MLV-NA), we quantitatively determined the sorting efficiency. For this purpose, we took samples of our emulsified particle mixtures (MLV-tPA and MLV-NA in a ratio of 1:100 and 1:1000) before and after sorting, recovered the virally packaged RNA, and performed a reverse transcription step. The resulting cDNA was subsequently quantified by real-time PCR (Figure 4D). Although before the sorting step the ratio of MLV-tPA/MLV-NA cDNA was only 4.4:100 (1:100) and 0.5:100 (1:1000), after sorting, this ratio increased to 7.9:1 (1:100) and 8.3:1 (1:1000). This corresponds to enrichment factors of 172-fold (1:100) and 1383-fold (1:1000) during a single selection round. The higher enrichment observed with the 1:1000 mixture is consistent with the previous observation that the sorter has a very low false positive error rate ( $<1$  in  $10^4$  droplets) and that the primary limit to enrichment is co-encapsulation (of viral particles in this case) in droplets (Baret et al., 2009): the predicted

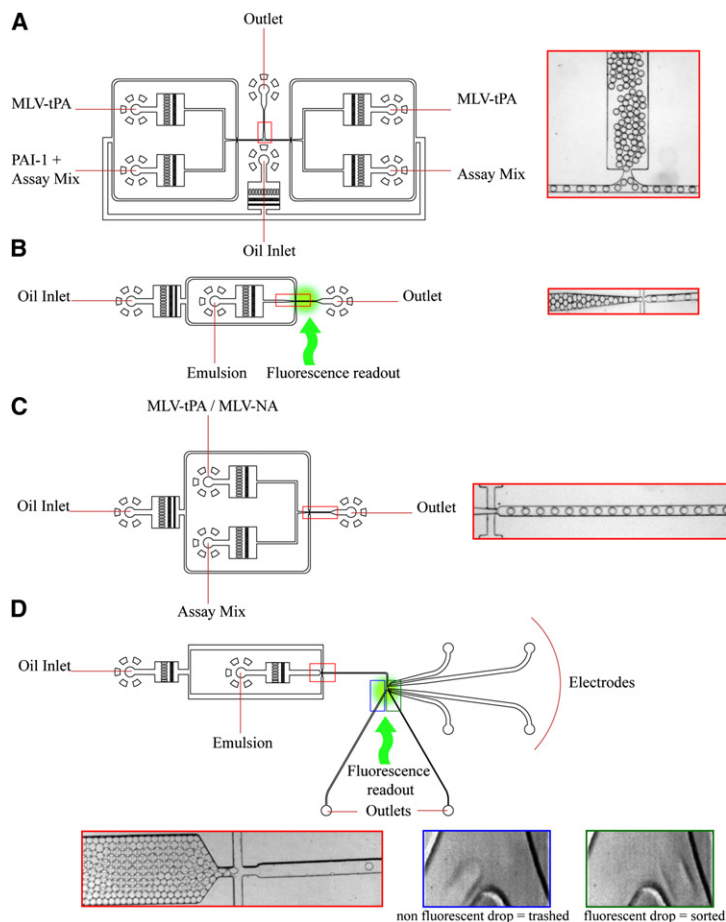


**Figure 2. Microfluidic Devices**

(A) Twin drop maker for the generation of emulsions with two different droplet species ( $\pm$ inhibitors).

(B) Reinjection device for fluorescence measurements.

(C) Drop maker for the encapsulation of particle mixtures.

(D) Sorting device. The geometry of the sorting module was calculated as described previously (Baret et al., 2009). Green spots indicate the focus of the laser beam for the fluorescence measurements. Colored rectangles indicate the sections shown in the microscopic images. On-chip filters are located after each inlet on all devices (Figure S4).

## DISCUSSION

We present here a novel approach for high-throughput screening of displayed enzymes. This method allows the selection of active variants under multiple turnover conditions, including eukaryotic enzymes that require complex post-translational modifications.

Displaying the enzyme of interest, tPA, on MLV particles not only ensured its expression in a eukaryotic context but also allowed highly efficient incorporation. Comparing the enzymatic activity of MLV-tPA at a defined particle titer (as determined during the encapsulation experiments) with that of soluble recombinant enzyme leads to the conclusion that, on average, 818 tPA molecules were displayed on the surface of each virion (Supplemental Information S5). Hence our display construct showed incorporation rates similar to that of homologous envelope proteins, of which normally several hundred are present on the particle surface (Bachrach et al., 2000; Chertova et al., 2002). In contrast, usually no more than one to five copies of an enzyme can be displayed on phage particles (Fernandez-Gacio et al., 2003), for which reason the MLV system used here seems to be beneficial. The size of libraries that can be screened is, however, a limiting factor. For non-replication competent MLV particles, mutated libraries comprising  $\sim 10^6$  protein variants have been described (Merten et al., 2006, 2005; Tolstrup et al., 2001), and a library of this diversity would take  $\sim 2$  hr to screen using the microfluidics system described here. This is significantly less than what can be selected using phage display (up to  $10^{12}$  variants) (Levin et al., 2006). Furthermore, the display of intracellular proteins on the surface of retroviruses has not yet been shown. However, this is most likely not a fundamental problem, but rather due to the fact that, to date, the generation of retroviral display libraries was mainly focusing on the engineering of viral envelope proteins with improved host cell tropisms for gene therapy purposes (Buchholz et al., 2008).

A strong advantage of the MLV system in comparison with cell-based eukaryotic display systems [e.g., yeast cell surface display (Shusta et al., 1999)] is that the enzyme of interest can be screened in absence of cellular enzymes (potentially causing significant background activities). MLV consists of just eight different proteins, thus minimizing the chance for any undesired background activities. Indeed, tPA-negative particles (MLV-NA)

enrichments, calculated assuming no sorting errors, are 306-fold and 3033-fold for the 1:100 and 1:1000 dilution, respectively, and are thus only  $\sim 2$ -fold higher than the experimentally observed enrichments. In general, higher enrichments are observed when the ratio of positive to negative particles is low. Furthermore, the reduction of the average number of particles per droplet to below 0.3 should allow higher enrichments at the expense of lower throughput (Baret et al., 2009).

As an alternative strategy to the amplification of virally packaged genes by RT-PCR, we also assessed the transduction of host cells and subsequent amplification based on cell proliferation. For this purpose we generated tPA particles co-displaying the G protein of the vesicular stomatitis virus (VSV-G) on their surface. While this did not significantly alter the enzymatic activity, it enabled the efficient transduction of HEK293T cells (titer of  $1.3 \times 10^5 \pm 9.9 \times 10^3$  i.U./ml). This approach should enable the initiation of a further selection cycle after the sorting step without the need for any subcloning, as with phage display and cell surface display technologies: transduced cells can be selected specifically by puromycin treatment (a resistance to this antibiotic is encoded on the viral vector) before being transfected with plasmids encoding the viral core proteins (to generate new particles displaying the selected enzymes). This should be useful for the screening of diverse enzyme libraries, allowing several selection rounds to be performed rapidly and consecutively.

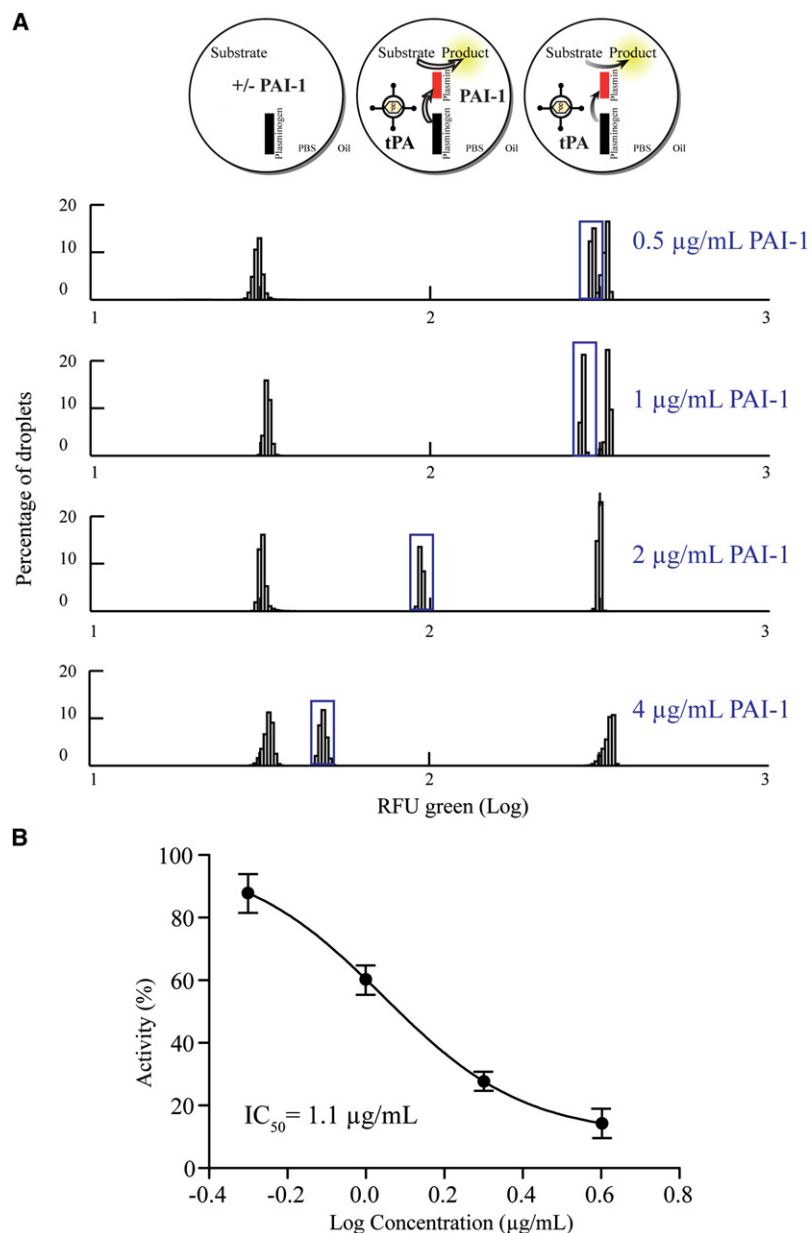


**Figure 3. Fluorescence Signals of Droplets Containing MLV-tPA Particles in the Presence of Different Concentrations of the Endogenous Inhibitor PAI-1 ( $\mu\text{g/mL}$ )**

(A) For each inhibitor concentration, three different droplet species were generated: empty droplets (lowest fluorescence; top left), droplets containing MLV-tPA in presence of the indicated inhibitor concentration (intermediate fluorescence; top center and highlighted by blue frames), and droplets containing MLV-tPA in absence of any inhibitor (highest fluorescence; top right). All fluorescence signals were normalized in respect to the droplets containing MLV-tPA in the absence of any inhibitor (highest fluorescence). The fluorescence signal (x axis, logarithmic scale) and the percentage of events (y axis) are shown for each inhibitor concentration.

(B) Mean enzymatic activity (y axis) from three independent experiments for each inhibitor concentration (x axis) (calculated using the mean activity from each independent experiment). The error bars correspond to the standard deviation of the mean. The IC<sub>50</sub> concentration was calculated using non-linear regression to fit the four parameter Hill Equation using GraphPad Prism.

quantitative measurements as demonstrated here (the IC<sub>50</sub> of the tPA inhibitor PAI-1 measured in droplets and in microtiter plates was almost identical). Second, fluorescence-activated droplet sorting in microfluidic systems has a very low sorting error rate ( $<10^{-4}$ ) and can be performed at rates of up to two kilohertz (Baret et al., 2009).

Quantitative enzyme screens can also be performed under multiple turnover conditions in microtiter plates; however, time and cost considerations generally limit the number of variants that can be screened to  $10^3$ – $10^5$ . Even using sophisticated robots, it is only possible to process 100,000 assays a day, or  $\sim 1$  per second, and it is difficult to reduce the assay volume below 1  $\mu\text{l}$  due to problems related to evaporation and capillary forces (Dove, 1999). In contrast, the droplet-based system allows the quantitative analysis of up to 500 samples per second (corresponding to  $4.3 \times 10^7$  samples per day), a throughput over 100 times higher than with microtiter plates. Furthermore, the assay miniaturization gives rise to massively reduced screening costs. When using 12  $\mu\text{l}$  droplets (as demonstrated here), the assay volumes are decreased approximately  $10^6$ -fold in comparison to microtiter plates (assuming an assay volume of 10  $\mu\text{l}$ ). This means that the consumables cost for screening  $10^7$  tPA variants is reduced from at least \$4,500,000 to only \$5.2, a nearly  $10^6$ -fold reduction (Supplemental Information S6).

## SIGNIFICANCE

**This manuscript describes a microfluidic approach for the screening of structurally complex enzyme variants. Similar to phage display, the enzyme variants are displayed on the**

mediated only a very low signal in the (bulk) fluorescence assay, whereas tPA-negative cells (HEK293T) generated significant fluorescence (S2).

In general, our method should be of special interest for the optimization of mammalian enzymes in clinical use, such as anticoagulants (tPA and urokinase), enzymes in cancer therapy (pegaspargase and rasburicase), or enzymes for the treatment of genetic diseases (pegademase, alglucerase, and dornase  $\alpha$ ). In contrast to conventional display techniques, the compartmentalization approach allows screens to be performed under multiple turnover conditions and enables the use of soluble substrates and products. Especially when using microfluidic devices for the generation and sorting of droplets, this approach seems to be extremely powerful. First, the droplets generated using microfluidic devices are highly monodisperse, allowing

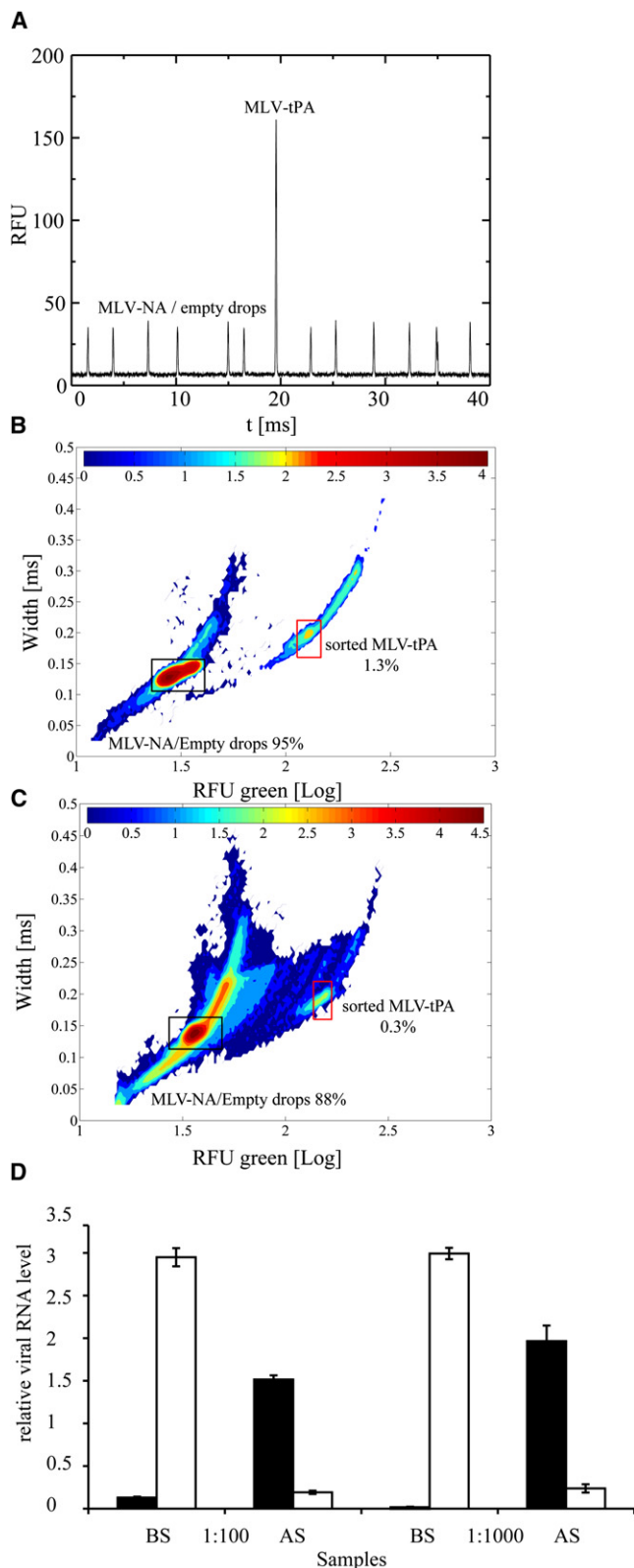


**Figure 4. Specific Sorting of Particles Displaying Active Enzyme Variants**

MLV-tPA and MLV-NA particles were mixed, encapsulated, and subjected to fluorescence-activated droplet sorting.

surface of viral particles. However, by using a mammalian expression system and encapsulating the resulting viral particles into tiny droplets (picoliter volumes), our approach enables the screening of structurally complex enzymes (e.g., requiring glycosylation and/or membrane anchorage) under multiple turnover conditions. In comparison to conventional screening formats such as microtiter plates, our system allows more than 100-fold increased throughput and almost one million-fold reduced consumables costs (due to the tiny assay volumes).

#### SUPPLEMENTAL INFORMATION

Supplemental Information includes four figures and Supplemental Experimental Procedures and can be found with this article online at doi:10.1016/j.chembiol.2010.02.011.

#### ACKNOWLEDGMENTS

The authors would like to thank D. Lieber for the kind donation of the plasmid pMSCV-puro-NA, Dr. A. El Harrak for advice with the synthesis of surfactants, and A. Alioua for advice and help with the qPCR. L.G. was supported by an Aide a la Formation et a la Recherche grant from the Fonds National de la Recherche (Luxembourg). J.-C.B. was supported by a European Molecular Biology Organization long-term fellowship and by the European Commission Framework Programme 6 MiFem Network. C.A.M. was supported by a Liebig Grant of the Fonds der Chemischen Industrie. This work was also supported by the Ministère de l'Enseignement Supérieur et de la Recherche, Fondation Recherche Médicale, Centre National de la Recherche Scientifique, and Agence Nationale de la Recherche (ANR-05-BLAN-0397).

Received: August 17, 2009

Revised: January 19, 2010

Accepted: February 11, 2010

Published: March 25, 2010

#### REFERENCES

- Aharoni, A., Griffiths, A.D., and Tawfik, D.S. (2005). High-throughput screens and selections of enzyme-encoding genes. *Curr. Opin. Chem. Biol.* 9, 210–216.
- Ahn, K., Kerbage, C., Hunt, T.P., Westervelt, R.M., Link, D.R., and Weitz, D.A. (2006). Dielectrophoretic manipulation of drops for high-speed microfluidic sorting devices. *Appl. Phys. Lett.* 88, 24104.
- Bachrach, E., Marin, M., Pelegrin, M., Karavanas, G., and Piechaczyk, M. (2000). Efficient cell infection by Moloney murine leukemia virus-derived

(A) Time sequence (x axis) and fluorescence (y axis) of droplets passing the laser beam (as shown in Figure 2D). Monitoring the droplet width (the time required for each droplet to pass the laser beam) allowed coalesced droplets (showing an increased width) to be excluded from the sort.

(B) Sorting of the 1:100 (MLV-tPA/MLV-NA) mixture. The sorting gate (red rectangle) was set to include only droplets with high fluorescence (x axis, logarithmic scale) and a width (y axis) indicating no coalescence. The black rectangle indicates the negative population. The percentage of total droplets in the gates is indicated. The color bar corresponds to the number of droplets on a logarithmic scale.

(C) Sorting of the 1:1000 (MLV-tPA/MLV-NA) mixture.

(D) Analysis of the sorting efficiency. Genetic markers recovered from the emulsions before (BS) and after the sort (AS) were reverse transcribed and quantified by real-time PCR. Black bars, tPA-encoding genes; white bars, NA-encoding genes. The error bars correspond to the standard deviation of the mean.

- particles requires minimal amounts of envelope glycoprotein. *J. Virol.* **74**, 8480–8486.
- Baret, J.C., Miller, O.J., Taly, V., Ryckelynck, M., El-Harrak, A., Frenz, L., Rick, C., Samuels, M.L., Hutchison, J.B., Agresti, J.J., et al. (2009). Fluorescence-activated droplet sorting (FADS): efficient microfluidic cell sorting based on enzymatic activity. *Lab Chip* **9**, 1850–1858.
- Beck, Z.Q., Hervio, L., Dawson, P.E., Elder, J.H., and Madison, E.L. (2000). Identification of efficiently cleaved substrates for HIV-1 protease using a phage display library and use in inhibitor development. *Virology* **274**, 391–401.
- Binz, H.K., Stumpp, M.T., Forrer, P., Amstutz, P., and Pluckthun, A. (2003). Designing repeat proteins: well-expressed, soluble and stable proteins from combinatorial libraries of consensus ankyrin repeat proteins. *J. Mol. Biol.* **332**, 489–503.
- Boder, E.T., and Wittrup, K.D. (1997). Yeast surface display for screening combinatorial polypeptide libraries. *Nat. Biotechnol.* **15**, 553–557.
- Buchholz, C.J., Peng, K.W., Morling, F.J., Zhang, J., Cosset, F.L., and Russell, S.J. (1998). In vivo selection of protease cleavage sites from retrovirus display libraries. *Nat. Biotechnol.* **16**, 951–954.
- Buchholz, C.J., Duerner, L.J., Funke, S., and Schneider, I.C. (2008). Retroviral display and high throughput screening. *Comb. Chem. High Throughput Screen.* **11**, 99–110.
- Chertova, E., Bess, J.W., Jr., Crise, B.J., Sowder, I.R., Schaden, T.M., Hilburn, J.M., Hoxie, J.A., Benveniste, R.E., Lifson, J.D., Henderson, L.E., et al. (2002). Envelope glycoprotein incorporation, not shedding of surface envelope glycoprotein (gp120/SU), is the primary determinant of SU content of purified human immunodeficiency virus type 1 and simian immunodeficiency virus. *J. Virol.* **76**, 5315–5325.
- Clausell-Tormos, J., Lieber, D., Baret, J.C., El-Harrak, A., Miller, O.J., Frenz, L., Blouwolf, J., Humphry, K.J., Koster, S., Duan, H., et al. (2008). Droplet-based microfluidic platforms for the encapsulation and screening of mammalian cells and multicellular organisms. *Chem. Biol.* **15**, 427–437.
- Demartis, S., Huber, A., Viti, F., Lozzi, L., Giovannoni, L., Neri, P., Winter, G., and Neri, D. (1999). A strategy for the isolation of catalytic activities from reporters of enzymes displayed on phage. *J. Mol. Biol.* **286**, 617–633.
- Dove, A. (1999). Drug screening—beyond the bottleneck. *Nat. Biotechnol.* **17**, 859–863.
- Fernandez-Gacio, A., Uguen, M., and Fastrez, J. (2003). Phage display as a tool for the directed evolution of enzymes. *Trends Biotechnol.* **21**, 408–414.
- Francisco, J.A., Campbell, R., Iverson, B.L., and Georgiou, G. (1993). Production and fluorescence-activated cell sorting of *Escherichia coli* expressing a functional antibody fragment on the external surface. *Proc. Natl. Acad. Sci. USA* **90**, 10444–10448.
- Griffiths, A.D., and Tawfik, D.S. (2006). Miniaturising the laboratory in emulsion droplets. *Trends Biotechnol.* **24**, 395–402.
- Hanes, J., and Pluckthun, A. (1997). In vitro selection and evolution of functional proteins by using ribosome display. *Proc. Natl. Acad. Sci. USA* **94**, 4937–4942.
- Hansson, L.O., Widersten, M., and Mannervik, B. (1997). Mechanism-based phage display selection of active-site mutants of human glutathione transferase A1-1 catalyzing SNAr reactions. *Biochemistry* **36**, 11252–11260.
- Levin, A.M., and Weiss, G.A. (2006). Optimizing the affinity and specificity of proteins with molecular display. *Mol. Biosyst.* **2**, 49–57.
- Levin, A.M., Coroneus, J.G., Cocco, M.J., and Weiss, G.A. (2006). Exploring the interaction between the protein kinase A catalytic subunit and caveolin-1 scaffolding domain with shotgun scanning, oligomer complementation, NMR, and docking. *Protein Sci.* **15**, 478–486.
- Lipovsek, D., Antipov, E., Armstrong, K.A., Olsen, M.J., Kilbanov, A.M., Tidor, B., and Wittrup, K.D. (2007). Selection of horseradish peroxidase variants with enhanced enantioselectivity by yeast surface display. *Chem. Biol.* **14**, 1176–1185.
- Mastrobattista, E., Taly, V., Chanudet, E., Treacy, P., Kelly, B.T., and Griffiths, A.D. (2005). High-throughput screening of enzyme libraries: in vitro evolution of a beta-galactosidase by fluorescence-activated sorting of double emulsions. *Chem. Biol.* **12**, 1291–1300.
- Merten, C.A., Stitz, J., Braun, G., Poeschla, E.M., Cichutek, K., and Buchholz, C.J. (2005). Directed evolution of retrovirus envelope protein cytoplasmic tails guided by functional incorporation into lentivirus particles. *J. Virol.* **79**, 834–840.
- Merten, C.A., Stitz, J., Braun, G., Medvedovska, J., Cichutek, K., and Buchholz, C.J. (2006). Fusoselect: cell-cell fusion activity engineered by directed evolution of a retroviral glycoprotein. *Nucleic Acids Res.* **34**, e41.
- Nikles, D., Bach, P., Boller, K., Merten, C.A., Montrasio, F., Heppner, F.L., Aguzzi, A., Cichutek, K., Kalinke, U., and Buchholz, C.J. (2005). Circumventing tolerance to the prion protein (PrP): vaccination with PrP-displaying retrovirus particles induces humoral immune responses against the native form of cellular PrP. *J. Virol.* **79**, 4033–4042.
- Olsen, M.J., Stephens, D., Griffiths, D., Daugherty, P., Georgiou, G., and Iverson, B.L. (2000). Function-based isolation of novel enzymes from a large library. *Nat. Biotechnol.* **18**, 1071–1074.
- Qiu, J., Swartz, J.R., and Georgiou, G. (1998). Expression of active human tissue-type plasminogen activator in *Escherichia coli*. *Appl. Environ. Microbiol.* **64**, 4891–4896.
- Roberts, R.W., and Szostak, J.W. (1997). RNA-peptide fusions for the in vitro selection of peptides and proteins. *Proc. Natl. Acad. Sci. USA* **94**, 12297–12302.
- Shusta, E.V., Kieke, M.C., Parke, E., Kranz, D.M., and Wittrup, K.D. (1999). Yeast polypeptide fusion surface display levels predict thermal stability and soluble secretion efficiency. *J. Mol. Biol.* **292**, 949–956.
- Soumillion, P., Jespers, L., Bouchet, M., Marchand-Brynaert, J., Winter, G., and Fastrez, J. (1994). Selection of beta-lactamase on filamentous bacteriophage by catalytic activity. *J. Mol. Biol.* **237**, 415–422.
- Tawfik, D.S., and Griffiths, A.D. (1998). Man-made cell-like compartments for molecular evolution. *Nat. Biotechnol.* **16**, 652–656.
- Tolstrup, A.B., Duch, M., Dalum, I., Pedersen, F.S., and Mouritsen, S. (2001). Functional screening of a retroviral peptide library for MHC class I presentation. *Gene* **263**, 77–84.
- Vanwetswinkel, S., Avalle, B., and Fastrez, J. (2000). Selection of beta-lactamases and penicillin binding mutants from a library of phage displayed TEM-1 beta-lactamase randomly mutated in the active site omega-loop. *J. Mol. Biol.* **295**, 527–540.
- Walsh, G., and Jefferis, R. (2006). Post-translational modifications in the context of therapeutic proteins. *Nat. Biotechnol.* **24**, 1241–1252.
- Yu, Y., and Wong, P.K. (1992). Studies on compartmentation and turnover of murine retrovirus envelope proteins. *Virology* **188**, 477–485.